Cloning, expression and characterisation of CYP102A2, a self-sufficient P450 monooxygenase from *Bacillus subtilis*

M. Budde, S. C. Maurer, R. D. Schmid, V. B. Urlacher *

Institute of Technical Biochemistry, Stuttgart University, Allmandring 31, 70569 Stuttgart, Germany

* Corresponding author:

Tel: +49-(0)711-685-4523; Fax: +49-(0)711-685-3196; e-mail: itbvur@itb.uni-stuttgart.de

Abstract

The gene encoding CYP102A2, a novel P450 monooxygenase from *Bacillus subtilis,* was cloned and expressed in *Escherichia coli.* The recombinant enzyme formed was purified by immobilised metal chelat affinity chromatography (IMAC) and characterised. CYP102A2 is a 119 kDa self-sufficient monooxygenase, consisting of an FMN/FAD–containing reductase domain and a heme domain. The deduced amino acid sequence of CYP102A2 exhibits a high level of identity with the amino acid sequences of CYP102A1 from *Bacillus megaterium* (59%) and CYP102A3 from *Bacillus subtilis* (60%). In reduced, CO-bound form, the enzyme shows a typical Soret band at 450 nm. It catalyses the oxidation of even- and odd-chain saturated and unsaturated fatty acids. In all reactions investigated, the products were the respective ω-3, ω-2 and ω-1 hydroxylated fatty acids. Activity was highest towards oleic and linoleic acid (K_M=17.4 ± 1.4 μM, k_{cat}= 2244 ± 72 min^{-1}), linoleic acid (K_M=12.25 ± 1.8 μM, k_{cat}= 1950 ± 84 min^{-1}). Comparison of CYP102A2 homology model to CYP102A1 crystal structure revealed significant differences in the substrate access channels, which might explain the differences in catalytic properties of these two enzymes.

Introduction

Cytochrome P450 monooxygenases (P450s or CYPs) are heme-containing proteins present in all kingdoms of life (Lewis 1996). CYPs play a pivotal role in the synthesis and metabolism of secondary metabolites such as prostaglandins (Berg et al. 2003), leucotrienes and thromboxanes (Kupfer & Holm 1989), steroid hormones (el-Monem et al. 1972, Sallam et al. 1977), insect and plant hormones (Durst & O'Keefe 1995, Feyereisen 1999), or colors and odours in plants (Holton et al. 1993). P450 monooxygenases in mammalian liver function as a biological defence system (Goldstein & Faletto 1993), which activate water-insoluble or barely water-soluble compounds for further degradation and elimination. As CYPs are able to introduce molecular oxygen regiospecifically and enantioselectively into allylic positions,

double bonds, or even into non-activated C-H bonds, they have recently been targeted as biocatalysts for the industrial production of fine chemicals such as pharmaceuticals or polymer building blocks. From a technical point of view, bacterial CYPs are more promising than those from plants and animals, as they are mostly soluble and not membrane-associated. They also show much higher reaction rates compared to CYPs from other sources, and they exhibit a relatively high stability. Activity and selectivity of bacterial CYPs can effectively be changed or/and improved by methods of site-directed mutagenesis or directed evolution (Appel et al. 2001, Salazar et al. 2003, Seng Wong et al. 2004). Great efforts are presently being made to improve storage and operational stability of bacterial P450 enzymes (e.g. tolerance towards organic solvents or hydrogen peroxide) (Maurer et al. 2003, Salazar et al. 2003, Seng Wong et al. 2004).

Among the members of the cytochrome P450 family, the monooxygenase from *Bacillus megaterium* (CYP102A1 or P450 BM-3) exhibits the highest turnover frequency (> 1000 min^{-1}). It is a catalytically self-sufficient monooxygenase, which contains a heme domain and a flavin reductase domain on a single polypeptide chain (Narhi & Fulco 1986, Wen & Fulco 1987), whereas the electron transport chain from NAD(P)H to heme iron in most CYPs involves separate electron transport proteins. From a technical point of view, such self-sufficient bacterial P450 monooxygenases facilitate *in vitro* applications as they do not require any separately added electron transport partners for function.

Analysis of the genome of the gram-positive bacterium *Bacillus subtilis* (Kunst et al. 1997) revealed eight candidate genes, which are potentially coding for P450 monooxygenases. Two of these genes - CYP102A2 and CYP102A3 - code for single-peptide monooxygenases, comprising both a heme and an FAD/FMN-containing reductase domain, and demonstrate a notable sequence similarity to CYP102A1. CYP102A3 has already been successfully cloned, expressed, characterised and modified through site-directed mutagenesis in our laboratory

(Lentz et al. 2003). CYP102A3 is involved in hydroxylation of unsaturated, saturated and branched chain fatty acids (Gustafsson et al. 2001, Lentz et al. 2004).

We now report the cloning, heterologous expression and characterisation of CYP102A2 from *Bacillus subtilis* with a focus on its substrate spectrum, kinetic parameters and stability. The products of this enzyme - hydroxylated or epoxidised fatty acids and their derivatives, especially if enantiomerically pure - might find applications in the preparation of fine chemicals for the synthesis of polymers, flavours, fragrances or pharmaceuticals.

Materials and methods

Chemicals

All chemicals were of analytical grade or higher quality and were purchased from Fluka (Buchs, Switzerland) or Sigma (Deisenhofen, Germany). Odd carbon number fatty acids were obtained from Cognis (Düsseldorf, Germany).

Strains, plasmids and growth conditions

E. coli strain DH5α (F^-; *supE44*; *lacU169*; [Φ80d *lacZ M15*] *hsdR17; recA1; endA1*) was purchased from Clontech (Palo Alto, USA.), *E. coli* strain BL21(DE3) (B; F^-; *omp*T *hsd*S_B (r_B^- m_B^-); *dcm; galλ*(DE3)) and the pET28b+ vector were purchased from Novagen (Madison, USA) and *Bacillus subtilis* strain 168 from the Deutsche Sammlung von Mikroorganismen und Zellkulturen (DSMZ 402). *E. coli* strains were grown at 37°C and shaking (150 rpm) in Luria Bertani (LB) or Terrific Broth (TB) medium supplemented with 30 µg/ml kanamycin. *Bacillus subtilis* was cultivated in LB medium at 30°C and shaking at150 rpm over night.

Cloning of *cyp*102A2 gene (yfnJ gene) from *Bacillus subtilis*

Genomic DNA from *Bacillus subtilis* was obtained by phenol / chloroform extraction and subsequent isopropanol precipitation. Amplification of the gene was performed by PCR using two oligonucleotide primers 5'-GAT*GGATCC*TATGAAGGAAACAAGCCCGAT-3' and 5'-CTA*GAGCTC*TTATATCCCTGCCCAGACATC-3'. Nucleotides in italics represent *Bam*HI and *Sac*I restriction sites, which will be introduced upstream of the *cyp*102A2 start codon and downstream of the stop codon. The PCR fragment was digested with *Bam*HI and *Sac*I and ligated into the corresponding site of the dephosphorylated pET28b+ vector resulting in pET28CYP102A2. *E. coli* transformed with pET28b+ were plated on LB agar containing 30 µg/ml kanamycin. The integrity of the cloned *cyp*102A2 gene was verified by DNA sequencing.

Expression and purification of CYP102A2

Cultures were grown in 2-liter flasks containing 400 ml TB medium supplemented with 30 µg/ml kanamycin at 37°C and shaking (150 rpm). At an optical density (OD_{578}) of 1.0 the expression was induced by 1 mM IPTG and 0.5 mM of the heme-precursor δ-aminolevulinic acid was added. Expression was carried out at 25°C and shaking (120rpm) over night. Cells were harvested by centrifugation at 10000*g for 20 min at 4°C and resuspended in 50 mM potassium phosphate buffer (pH 7.5), containing 500 mM sodium chloride, 5 mM imidazole and 0.1 mM phenylmethylsulfonyl fluoride (PMSF). Cells were disrupted by sonication on ice (5 x 1 min, output control 4, duty cycle 40%, Branson Sonifier W250, Dietzenbach, Germany) and the cell debris was removed by centrifugation at 37000*g for 30 min. The N-terminally attached His_6-tag allows purification by immobilised metal chelate affinity chromatography (IMAC) utilising a Ni-NTA-resin (Qiagen, Germany). The column-bound enzyme was washed with 50 mM potassium phosphate buffer (pH 7.5) containing 500 mM sodium chloride and 50 mM imidazole. Elution was performed by increasing the imidazole

concentration to 200 mM. Imidazole and sodium chloride were removed by dialysis against 50 mM potassium phosphate buffer (pH 7.5) over night. The purity of the enzyme was estimated by SDS-PAGE using 10% polyacrylamide running gels (Laemmli 1970). Enzyme samples were supplemented with 50% glycerol and stored at –20°C until use.

CYP102A2 concentration measurement and absorption spectra

Absorption spectra, NADPH oxidation and CO difference spectra were measured on an Ultrospec 3000 UV/vis–spectrometer (Amersham Biosciences, Sweden). CYP102A2 concentrations were measured based on reduced CO difference spectra using an extinction coefficient of 91 $mM^{-1} * cm^{-1}$ at 450 nm (Omura & Sato 1964). Absorption spectra showing substrate binding by the characteristic blue shift in the Soret band were recorded using 0.18 $nmol * ml^{-1}$ CYP102A2 in 500 µl 50 mM potassium phosphate buffer (pH 7.5) and 20 µl 5 mM oleic acid in DMSO and 50 mM potassium phosphate buffer as a reference.

Substrate screening

For substrate screening NADPH oxidation was measured by tracking the absorption decrease at 340 nm with an UV/vis-spectrometer. A solution containing 915 µl potassium phosphate buffer (pH 7.5), 10 µl 0.3 mM substrate solution in dimethylsulfoxide (DMSO) and 50 µl enzyme solution (c = 0.8 nmol/ml) was incubated for 5 min in a cuvette. The reaction was started by adding 75 µl of 10 mM NADPH solution. The reaction was monitored for 10 min.

For determination of kinetic parameters a substrate concentration range of 20 to 500 µM was used. To enhance substrate solubility 1 mM cholic acid was added to the reaction buffer. All values have been determined at least in triplicates.

The data were fitted to the Michaelis-Menten equation by linear regression.

Cytochrome c test

Reductase activity was determined by performing the standard cyctochrome c assay in microtiter plates using a Spectra max 340 microtiterplate UV/vis Spectrometer (Molecular Devices, Germany). 160 µl of a 3 nM CYP102A2 solution in 50 mM potassium phosphate buffer (pH 7.5) and 20 µl of a cytochrome c solution (c= 0.75 mg * ml^{-1} to c= 6 mg * ml^{-1}) in the same buffer were added to each well. The reaction was started by adding 20 µl 1 mM NADPH solution.

Activity and stability of CYP102A2

For determination of thermostability, the enzyme samples were incubated at different temperatures between 0°C and 60°C for 30 min. The residual activity was determined using NADPH oxidation assay as described above. Reductase domain stability was determined by measuring the fluorescence signal (excitation at 470 ± 6 nm, emission at 510 ± 5 nm) of enzyme samples preincubated at the respective temperatures. As the FAD and FMN fluorescence signals are quenched within the intact reductase, emission is only detectable when the apoprotein is formed by release of FAD and FMN.

Optimal reaction conditions in terms of pH value and temperature were determined with linoleic acid as a substrate by monitoring the NADPH oxidation.

Long term operational stability was measured using an amicon® ultrafiltration cell (model 8050, Amicon Division, USA) equipped with a regenerated cellulose membrane (MWCO 50 kDa). 0.3 nmol CYP102A2 in reaction buffer consisting of 0.3 µM *p*-nitrophenoxydodecanoic acid (12-*p*NCA), 0.5 mM NADPH and 2% DMSO in 1.2 ml 50 mM potassium phosphate buffer (pH 8.1) were added and the mixture was stirred gently. Samples of 1 ml were taken every 30 min. The removed volume was replaced by reaction buffer. The conversion of 12-*p*NCA was determined by measuring the absorption of *p*-nitrophenolate at 410 nm (Schwaneberg et al. 1999).

CYP102A2 - catalysed reactions and product derivatisation

Reaction solutions containing 700 µl 4 µM CYP102A2, 200 µl 100 mM substrate in DMSO, 8 ml 50 mM phosphate buffer (pH 7.5) and 1 ml 3 mM NADPH were stirred carefully at room temperature for 30 min. After addition of another 1 ml of 3 mM NADPH solution the reaction was continued for further 30 min. The solution was then acidified to pH 2-3 with diluted hydrochloric acid and extracted thrice with diethyl ether. The combined organic layers were dried over magnesium sulphate and the solvent was evaporated in vacuo. The residue was dissolved in 300 µl of a 1:1 mixture pyridine : N,O-bis(trimethylsilyl)trifluoroacetamide (BSTFA) + 1% (v/v) trimethylchlorosilane. The solution was transferred into a glass vial and incubated at 75°C for 30 min to yield trimethylsilylated products.

Product identification

Product analysis was carried out by GC/MS (Shimadzu GCMS-QP2010, column: FS-Supreme-5, length: 30 m, internal diameter: 0.25 mm, film thickness: 0.25 µm) using helium as carrier gas. Mass spectra were collected using electron ionisation. The column oven was programmed as follows: 200°C for one minute, 10°C per minute to 275°C. Product distribution and educt turnover were calculated from the peak area ratios.

Results

Cloning and overexpression of CYP102A2

The *cyp*102A2 gene was amplified from *Bacillus subtilis* genomic DNA by PCR using oligonucleotides, which were designed to introduce *Bam*HI and *Sac*I restriction sites. The *cyp*102A2 gene was cloned into pET28b+ vector resulting in expression plasmid pET28CYP102A2. The CYP102A2 monooxygenase with N-terminal His_6-tag was

heterologously expressed in *E. coli* BL21 (DE3) cells. Optimisation of the expression protocol by altering temperature, shaking speed, cultivation time and the concentration of inducer – IPTG − lead to expression of approximately 40 mg of CYP102A2 per litre of culture. Analysis of enzyme production in BL21 (DE3) cells by sodium dodecyl sulphate gel electrophoresis clearly revealed a band with the expected size of approximately 120 kDa. For a standard enzyme production the protocol described in materials and methods was used. CYP102A2 was purified on a nickel affinity resin using the facility of His_6-tag and subsequent dialysis procedure (Table 1). The protein recovery after purification was 32%. SDS-PAGE analysis revealed a thick protein band corresponding to our target protein at 120 kDa (Fig. 1) and minor impurities. However, the amount of CYP102A2 calculated from CO difference spectra towards the total protein concentration was only 28%. This can be explained by imidazole inhibition of the heme domain, which leads to a 30% inactivation of CYP102A2 detected by CO difference spectra even after dialysis against 50 mM potassium phosphate buffer. Besides that, not enough heme was produced and incorporated into the protein during expression, as shown by a 30% increase in CYP102A2 measured in CO difference spectra, when 0.5 mM of the heme precursor δ-aminolevulinic acid was added.

Characterisation of recombinant CYP102A2 monooxygenase

The protein was first examined by UV-visible spectroscopy (Fig. 2) that revealed the typical characteristics of P450, a heme Soret band at 418 nm (low spin) in the absence of substrate, which shifted to 392 nm (high spin) upon the addition of oleic acid. The broad absorbance shoulder between 450 and 510 nm is characteristic for a flavin containing reductase domain. Addition of NADPH to the enzyme solution resulted in the disappearance of this shoulder due to flavin (FAD and FMN) reduction. The spectrum of the dithionite-reduced and CO - bound form showed the well known absorption maximum at 449 nm.

Both NADPH and NADH were tested as possible electron donors. Cytochrome c reduction using NADPH was much faster than with NADH. In all further experiments, NADPH was used as an electron donor. Reductase activity of CYP102A2 towards cytochrome c (4180 min^{-1}) was higher than that reported for CYP102A1 (2900 min^{-1}) (Miles et al. 1992), whereas affinity was lower (K_M=28.5 ± 5.0 for CYP102A2, K_M=12.0 ± 3.0 for CYP102A1 (Noble et al. 1999)). Several classes of substrates like fatty acids, esters of fatty acids, alkanes, cycloalkanes, aromatic compounds and polycyclic aromatic compounds were tested as potential substrates of CYP102A2 (Table 2). For initial substrate screening, NADPH oxidation at 340 nm was measured. The only substrates found by this test were saturated and unsaturated fatty acids. Steady-state kinetic measurements revealed an unusual behaviour of CYP102A2 towards saturated fatty acids. Although turnover rates for myristic and palmitic acid were comparable to those of oleic and linoleic acid, affinity of saturated fatty acids to the enzyme was extremely poor: K_M values were 40-200 folds higher than for unsaturated fatty acids (Table 3). High standard deviations for kinetic parameters were observed with saturated fatty acids and might be explained by cooperative effects between several hypothetical substrate binding sites: in such case, reaction kinetics would not correspond to the classical Michaelis-Menten equation and dependency of reaction rate on substrate concentration has a sigmoidal behaviour (Fig. 3a). In the case of unsaturated fatty acids as oleic acid a typical hyperbolic profile, corresponding to Michaelis-Menten kinetics was observed (Fig. 3b).

Saturated fatty acids with carbon chain lengths less than C12 were not converted by CYP102A2. Lauric acid was hydroxylated by CYP102A2 with very low activity, which was difficult to quantify. The odd-chain fatty acid tridecanoic acid was hydroxylated with a turnover rate of 15 % compared to its even-chain higher homologue, myristic acid. (Fig. 4), but pentadecanoic acid turnover was nearly even to palmitic acid, and heptadecanoic acid was oxidised much faster than stearic acid. The turnover rate of myristic acid hydroxylation was

the highest among saturated fatty acids. Activity of the enzyme towards saturated fatty acids decreased gradually with higher carbon chain lengths.

The enzyme was unexpectedly active at high temperatures. Although isolated from a mesophilic soil bacterium, the enzyme showed highest activity at 51°C, even though its stability was dramatically reduced at this temperature. 30 min incubation at 31°C and 49°C resulted in 61% and 17 % residual activity, correspondingly. Incubation at 60°C led to total inactivation of the monooxygenase . The contribution of the reductase domain to the loss of activity was monitored by measuring fluorescence emission of liberated FAD/FMN, which started at 30°C and increased linearly until 60°C. Activity of CYP102A2 was highest at pH 7.0. Operational stability of CYP102A2 was determined using a simple model of an enzyme membrane reactor as described in the Materials and Methods section. CYP102A2 has a half-life of approximately 5 hours in a reaction with 12-*p*NCA at 23°C.

Product identification

All products were clearly identified by their characteristic MS fragmentation patterns. Three types of ions were used to determine the position of hydroxylation:

m/z=117 to 145 $[CH_3(CH2)_nCHOTMS]^+$ for myristic acid, pentadecanoic acid and oleic acid; m/z=345 to 373 $[TMSOCO(CH_2)_nCHOTMS]^+$ and m/z= 316 to 344 $[TMSOCO(CH_2)_nTMS]^+$ for myristic acid; m/z=359 to 373 $[TMSOCO(CH_2)_nCHOTMS]^+$ and m/z= 330 to 344 $[TMSOCO(CH_2)_nTMS]^+$ for pentadecanoic acid; m/z=399 to 427 $[TMSOCO(CH_2)_nCHOTMS]^+$ and m/z= 370 to 398 $[TMSOCO(CH_2)_nTMS]^+$ for oleic acid. Conversion of oleic acid, myristic acid and pentadecanoic acid by CYP102A2 leads to subterminal hydroxylation of the substrates as confirmed by GC/MS analyses. The chromatograms of myristic acid and oleic acid reaction extracts show a similar product

distribution of ω-1 to ω-3 hydroxylated fatty acids (ω-1 : ω-2 : ω-3 ≈ 1:2:1). For pentadecanoic acid equal amounts of the three regioisomeric products were found. Interestingly, CYP102A1 hydroxylates fatty acids preferably at ω-1 position. This fact can be explained by a structural discrepancy of the active sites and the substrate access channels of the two enzymes (see discussion).

Discussion

CYP102A2 from *Bacillus subtilis* was successfully cloned, expressed in *Escherichia coli* and purified via IMAC chromatography. The physical properties and the substrate spectrum of the enzyme were studied. The optimum temperature of 51°C proved surprisingly high, but the protein is rapidly inactivated at elevated temperatures. Due to the high amino acid sequence homology to CYP102A1 and to CYP102A3, both fatty acid hydroxylases, it is not surprising, that CYP102A2 also catalyses the conversion of fatty acids to their ω-3, ω-2 and ω-1 hydroxylated products. Even- and odd-chain as well as unsaturated fatty acids (myristic, pentadecanoic and oleic acid) were all exclusively hydroxylated at positions ω-3, ω-2 and ω-1.

Comparing the amino acid sequences of CYP102A1 and CYP102A2 as well as their structures (homology model of CYP102A2 generated with SWISS-PROT (Peitsch 1995, Guex & Peitsch 1997, Schwede et al. 2003) and crystal structure of CYP102A1 (Ravichandran et al. 1993, Li & Poulos 1997)) revealed some differences within the substrate access channel, which might explain the different regioselectivity and kinetic constants found for CYP102A2 (Fig 5). Arginine R47, located at the entrance of the active site of CYP102A1 interacts with the carboxylate group of the fatty acid substrate (Li & Poulos 1997) As shown by mutagenesis experiments at R47 and Y51 (Ost et al. 2000), both residues are crucial for the proper positioning of the substrate. In CYP102A2, residue 48 (homologous to R47 in

CYP102A1) is glycine, which rules out a direct effect on substrate binding. Our structural model of CYP102A2 leaves room to speculate that, instead, residue R353 might position the substrates, though in a weaker manner than the R47/Y51 couple of CYP102A1 as the stabilising hydrogen bond from tyrosine is missing. This model can explain the higher K_M values of CYP102A2 as compared to CYP102A1 towards identical substrates. However, mutagenesis experiments are clearly required to substantiate this hypothesis. Further investigations of this interesting novel P450 monooxygenase are now in progress. This includes the screening of mutants, obtained by site-directed mutagenesis and directed evolution.

Acknowledgments

We thank Dr. A. Weiss for providing us with odd-chain fatty acids and Dr. U. Hofmann for assistance in GC/MS analyses.

Reference

Appel D, Lutz-Wahl S, Fischer P, Schwaneberg U, Schmid RD (2001) A P450 BM-3 mutant hydroxylates alkanes, cycloalkanes, arenes and heteroarenes. J Biotechnol 88:167-171.

Berg JM, Tymoczko JL, Stryer L (2003) Biochemistry, Vol 5. W.H. Freeman and Company, New York

Durst F, O'Keefe DP (1995) Plant Cytochromes P450: An Overview. Drug Metab. Drug Interact 12:171-187

el-Monem A, el-Refai H, Sallam AR, Geith H (1972) Microbial 11 -hydroxylation of progesterone. Acta Microbiol Pol B 4:31-36

Feyereisen R (1999) Insect P450 Enzymes. Annu. Rev. Entomol. 44:507-533

Goldstein JA, Faletto MB (1993) Advances in Mechanisms of Activation and Deactivation of Environmental Chemicals. Environ. Health Perspect. 100:169-176

Guex N, Peitsch MC (1997) SWISS-MODEL and the Swiss-PdbViewer: an environment for comparative protein modeling. Electrophoresis 18:2714-2723

Gustafsson MC, Palmer CN, Wolf CR, von Wachenfeldt C (2001) Fatty-acid-displaced transcriptional repressor, a conserved regulator of cytochrome P450 102 transcription in Bacillus species. Arch Microbiol 176:459-464

Holton TA, Brugliera F, Lester DR, Tanaka Y, Hyland CD, Menting JG, Lu CY, Farcy E, Stevenson TW, Cornish EC (1993) Cloning and Expression of Cytochrome P450 Genes Controlling Flower Colour. Nature 366:276-279

Kunst F, Ogasawara N, Moszer I, Albertini AM, Alloni G, Azevedo V, Bertero MG, Bessieres P, Bolotin A, Borchert S, Borriss R, Boursier L, Brans A, Braun M, Brignell SC, Bron S, Brouillet S, Bruschi CV, Caldwell B, Capuano V, Carter NM, Choi SK, Codani JJ, Connerton IF, Danchin A, et al. (1997) The complete genome sequence of the gram-positive bacterium Bacillus subtilis. Nature 390:249-256

Kupfer D, Holm KA (1989) Prostaglandin Metabolism by Hepatic Cytochrome P450. Drug Metab. Rev. 20:753-764

Laemmli UK (1970) Cleavage of structural proteins during the assembly of the head of bacteriophage T4. Nature 227:680-685

Lentz O, Urlacher V, Schmid RD (2003) Substrate specificity of native and mutated cytochrome P450 (CYP102A3) from Bacillus subtilis. Journal Biotechnology accepted

Lentz O, Urlacher V, Schmid RD (2004) Comparison of CYP102A3 with CYP102A1. J Biotechnol in press

Lewis DF (1996) Cytochromes P450: Structure, Function and Mechanism, Vol 1, Vol. Taylor & Francis, London

Li H, Poulos TL (1997) The structure of the cytochrome p450BM-3 haem domain complexed with the fatty acid substrate, palmitoleic acid. Nat Struct Biol 4:140-146

Maurer S, Urlacher V, Schulze H, Schmid RD (2003) Immobilisation of P450 BM-3 and an NADP+ cofactor recycling system: towards a technical application of heme-containing monooxygenases in fine chemical synthesis. Adv Synth Catal 345:802-810

Miles JS, Munro AW, Rospendowski BN, Smith WE, McKnight J, Thomson AJ (1992) Domains of the catalytically self-sufficient cytochrome P-450 BM-3. Genetic construction, overexpression, purification and spectroscopic characterization. Biochem J 288 (Pt 2):503-509

Narhi LO, Fulco AJ (1986) Characterization of a catalytically self-sufficient 119,000-dalton cytochrome P-450 monooxygenase induced by barbiturates in Bacillus megaterium. J Biol Chem 261:7160-7169

Noble MA, Miles CS, Chapman SK, Lysek DA, MacKay AC, Reid GA, Hanzlik RP, Munro AW (1999) Roles of key active-site residues in flavocytochrome P450 BM3. Biochem J 339:371-379.

Omura T, Sato RJ (1964) The Carbon Monoxide-binding Pigment of Liver Microsomes. I Evidence for its Hemoprotein Nature. J. Biol. Chem. 239:2370-2378

Ost TW, Miles CS, Murdoch J, Cheung Y, Reid GA, Chapman SK, Munro AW (2000) Rational re-design of the substrate binding site of flavocytochrome P450 BM3. FEBS Lett 486:173-177

Peitsch MC (1995) Protein Modeling by E-Mail (Vol 13, Pg 658, 1995). Bio-Technology 13:723-723

Ravichandran KG, Boddupalli SS, Hasermann CA, Peterson JA, Deisenhofer J (1993) Crystal structure of hemoprotein domain of P450BM-3, a prototype for microsomal P450's. Science 261:731-736

Salazar O, Cirino PC, Arnold FH (2003) Thermostabilization of a Cytochrome P450 Peroxygenase. Chembiochem 4:891-893

Sallam L, Naim N, Zeinel-Abdin Badr A, El-Refai A (1977) Bioconversion of progesterone with cell preparations with Aspergillus niger 171. Rev Latinoam Microbiol 19:151-153

Schwaneberg U, Schmidt-Dannert C, Schmitt J, Schmid RD (1999) A continuous spectrophotometric assay for P450 BM-3, a fatty acid hydroxylating enzyme, and its mutant F87A. Anal Biochem 269:359-366

Schwede T, Kopp J, Guex N, Peitsch MC (2003) SWISS-MODEL: An automated protein homology-modeling server. Nucleic Acids Res 31:3381-3385

Seng Wong T, Arnold FH, Schwaneberg U (2004) Laboratory evolution of cytochrome p450 BM-3 monooxygenase for organic cosolvents. Biotechnol Bioeng 85:351-358

Wen LP, Fulco AJ (1987) Cloning of the gene encoding a catalytically self-sufficient cytochrome P-450 fatty acid monooxygenase induced by barbiturates in Bacillus megaterium and its functional expression and regulation in heterologous (Escherichia coli) and homologous (Bacillus megaterium) hosts. J Biol Chem 262:6676-6682

Tables

Table 1 Purification of CYP102A2

Purification step	Total protein (μg ml^{-1})	CYP102A2 (μg ml^{-1})	Yield (%)	Purification (fold)
Crude extract	5981	251	100	1
IMAC	1467	413	32	6.7

Table 2 Substrates screened towards activity with CYP102A2, NADPH consumption is given in $n(NADPH)*n(CYP102A2)^{-1}*min^{-1}$

Substrate	NADPH-consumption	Substrate	NADPH-consumption
capric acid	n.d.	n-octane	n.d.
undecanoic acid	n.d.	n-decane	n.d.
lauric acid	~10	n-dodecane	n.d.
dodecanedioic acid	n.d.	n-hexadecane	n.d.
tridecanoic acid	50	indazole	n.d.
myristic acid	334	indole	n.d.
pentadecanoic acid	240	naphthalene	n.d.
palmitic acid	249	anthracene	n.d.
heptadecanoic acid	148	acridine	n.d.
stearic acid	79	β-ionone	n.d.
oleic acid	846	2,6-lutidine	n.d.
linoleic acid	902	styrene	n.d.
3-hydroxy pyridine	n.d.	5-bromoindole	n.d.
carbazole	n.d.	12-*p*NCA	220

Table 3 Kinetic parameters for oxidation of fatty acids catalysed by CYP102A2

Substrate	K_M [μM]	k_{cat} [min^{-1}]	k_{cat}/K_M [$\mu M^{-1}*min^{-1}$]
oleic acid	17.36 ± 1.4	2244 ± 72	130 ± 14
linoleic acid	12.25 ± 1.8	1950 ± 84	160 ± 30
myristic acid	2152 ± 200	2334 ± 858	1.1 ± 0.5
palmitic acid	430 ± 100	2064 ± 60	4.8 ± 1.7

Figure legends

Fig. 1 SDS-PAGE analysis of CYP102A2 purification (10 μg of protein per lane). Lanes: 1 cell extract; 2 column flow-through fraction; 3 washing fraction; 4 purified CYP102A2; M molecular weight standard

Fig. 2 UV/vis absorption spectra of CYP102A2: oxidised CYP102A2 (dotted line); oxidised CYP102A2 plus oleic acid (dash-dotted line); NADPH reduced form (solid line); dithionite reduced and CO-bound form (dashed line)

Fig. 3 Dependence of NADPH oxidation rates on substrate concentration: A myristic acid as substrate; B oleic acid as substrate

Fig. 4 Activity of CYP102A2 towards different saturated fatty acids (100% activity = 700 nmol NADPH consumption per nmol CYP102A2 per minute as measured for myristic acid)

Fig. 5 Overlay of CYP102A2 (black) and CYP102A1 (grey) amino acids within the substrate access channel

Figure 1:

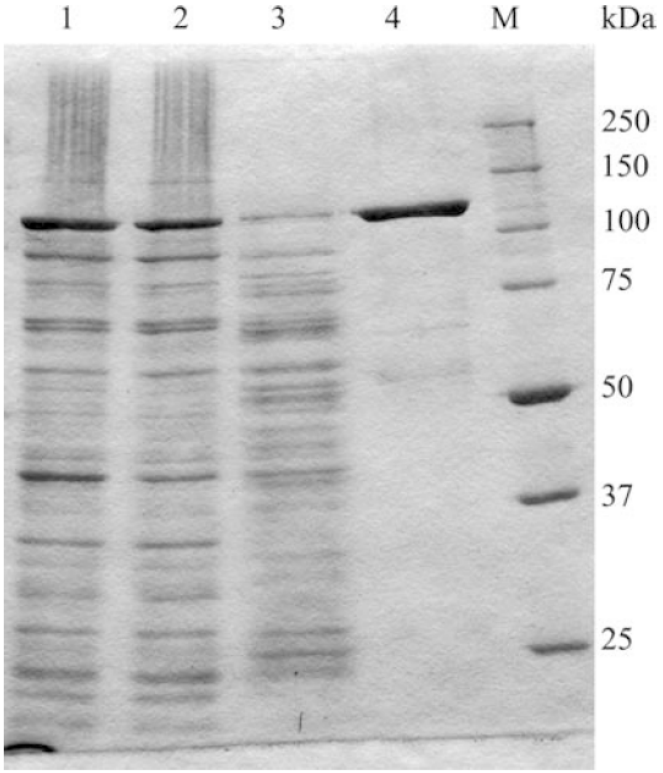

Figure 2:

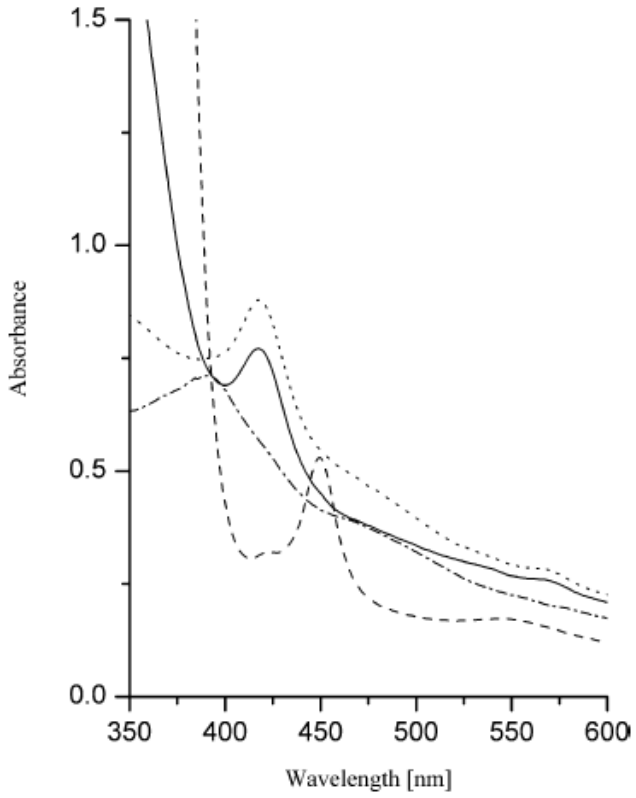

Figure 3:

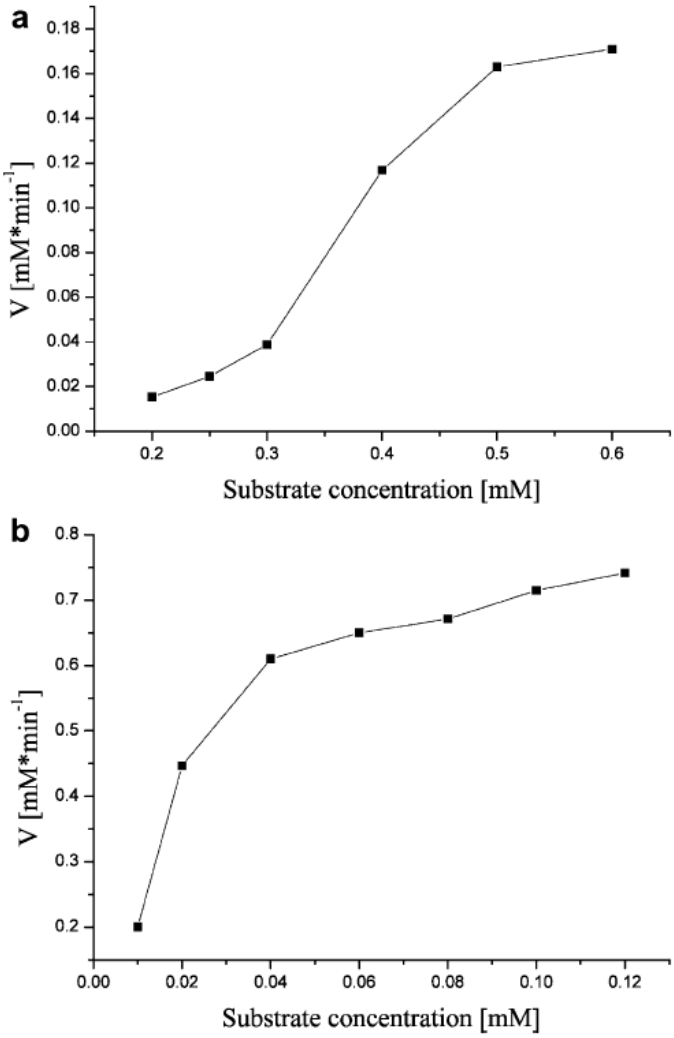

Figure 4:

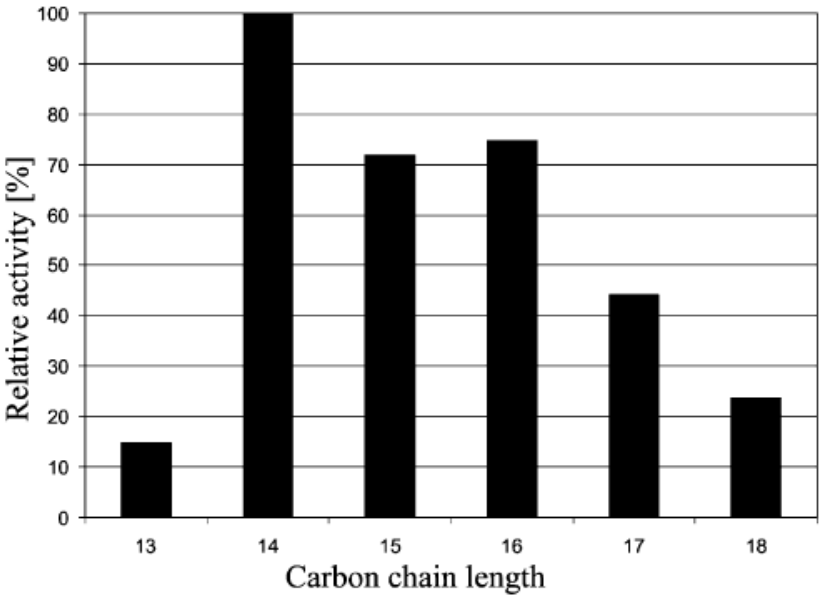

Figure 5: